AD-A090 976 HARRY DIAMOND LABS ADELPHI MD F/G 20/2
OPTICAL SPECTRA OF YB3+ IN CRYSTALS WITH SCHEELITE STRUCTURE. I--ETC(U)
SEP 80 E A BROWN
UNCLASSIFIED HDL-TR-1934 NL

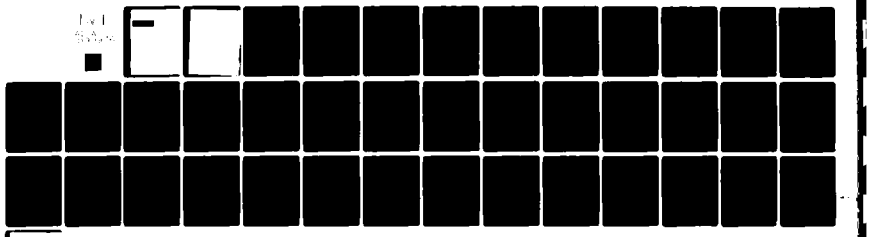

END
DATE FILMED
11-80
DTIC

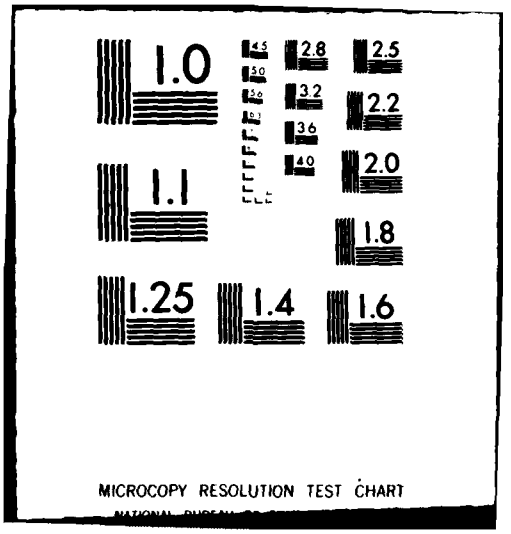
1.0
1.1
1.25
1.4
1.6
1.8
2.0
2.2
2.5
2.8
3.2
3.6
4.0
4.5
5.0
5.6
MICROCOPY RESOLUTION TEST CHART

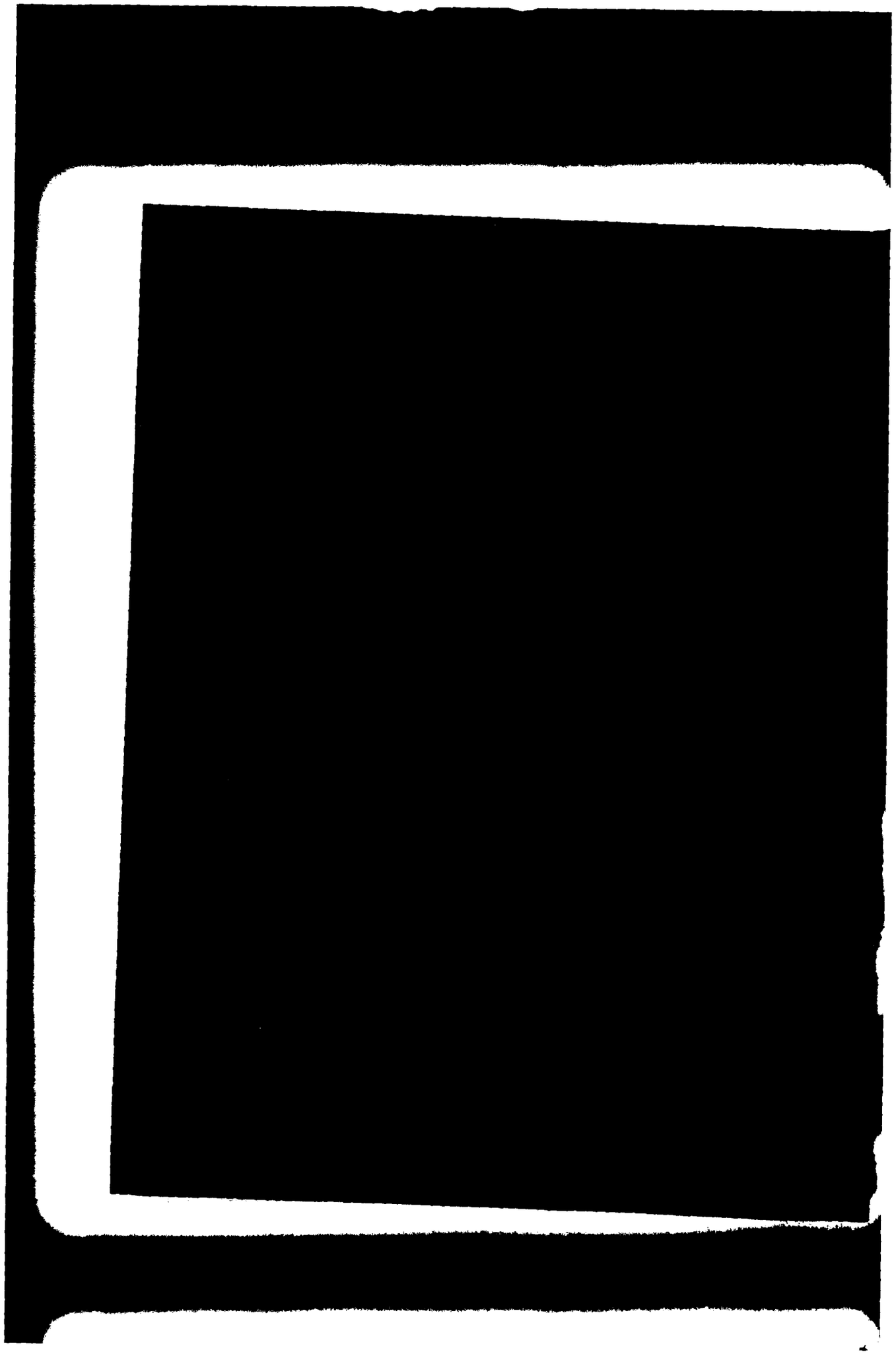

UNCLASSIFIED

SECURITY CLASSIFICATION OF THIS PAGE (When Data Entered)

REPORT DOCUMENTATION PAGE	READ INSTRUCTIONS BEFORE COMPLETING FORM
1. REPORT NUMBER: HDL-TR-1934	2. GOVT ACCESSION NO.: AD-A090976	3. RECIPIENT'S CATALOG NUMBER
4. TITLE (and Subtitle): Optical Spectra of Yb^{3+} in Crystals with Scheelite Structure. II. Crystal-Field Calculations and a Phenomenological Crystal-Field Model	5. TYPE OF REPORT & PERIOD COVERED: Technical Report
	6. PERFORMING ORG. REPORT NUMBER
7. AUTHOR(s): Edward A. Brown	8. CONTRACT OR GRANT NUMBER(s)
9. PERFORMING ORGANIZATION NAME AND ADDRESS: Harry Diamond Laboratories, 2800 Powder Mill Road, Adelphi, MD 20783	10. PROGRAM ELEMENT, PROJECT, TASK AREA & WORK UNIT NUMBERS: 12 38
11. CONTROLLING OFFICE NAME AND ADDRESS: US Army Materiel Development and Readiness Command, Alexandria, VA 22333	12. REPORT DATE: September 1980
	13. NUMBER OF PAGES: 39
14. MONITORING AGENCY NAME & ADDRESS (if different from Controlling Office)	15. SECURITY CLASS. (of this report): UNCLASSIFIED
	15a. DECLASSIFICATION/DOWNGRADING SCHEDULE

16. DISTRIBUTION STATEMENT (of this Report)

Approved for public release; distribution unlimited.

17. DISTRIBUTION STATEMENT (of the abstract entered in Block 20, if different from Report)

18. SUPPLEMENTARY NOTES

AIF appropriation: 21X4992.06LA 6L S18129
HDL Project: 001A14

19. KEY WORDS (Continue on reverse side if necessary and identify by block number)

Crystal fields
Scheelites
Rare earths
Laser materials
Lattice sums
Nephelauxetic effect
Covalent bonding

20. ABSTRACT (Continue on reverse side if necessary and identify by block number)

The optical and Zeeman spectra were reported for Yb^{3+} in nine single crystal scheelite hosts in a previous report. Identification of the S_4 spectral lines allowed the energy level schemes for Yb^{3+} in the nine scheelites to be determined. From this, best-fit sets of crystal-field parameters were calculated to fit the expansion of the crystal-field potential, $V_c = \Sigma B_n^m C_n^m$. The dependence of the B_n^m on the unit cell volume was examined, and it was found that the strength of the crystal field

DD FORM 1 JAN 73 1473 EDITION OF 1 NOV 65 IS OBSOLETE

UNCLASSIFIED

SECURITY CLASSIFICATION OF THIS PAGE (When Data Entered)

20. ABSTRACT (Cont'd)

as measured by the crystal-field parameters and the resulting Stark splitting decreased when the unit cell volume increased. It was found also that the dependence of the Stark splitting was more sensitive to the lower order parameters, B_2^0, B_4^0, and B_4^4, than to the higher order ones, B_6^0 and $B_6^{\pm 4}$, by almost an order of magnitude.

Crystal-field parameters were also calculated from first principles by using the conventional electrostatic point charge model, and the results of these calculations were compared with the empirically determined parameters. As had been found previously, agreement was poor with the discrepancies between experimental fit and calculation an order of magnitude or greater. Various phenomenological corrections to the point charge model were investigated including (1) adjustment of the ligand oxygen effective charge to account for the covalent nature of the heavy metal tetrahedron, (2) application of an effective dielectric constant depending exponentially on distance from the impurity ion to take into account the effects of lattice polarization, (3) expansion of the 4f radial wave function (nephelauxetic effect), and (4) reduction of the nearest neighbor (ligand) distance to account for the local lattice distortion due to the size discrepancy between the Yb^{3+} ion and the normal cation. Crystal-field parameters were calculated by adjusting various parameters to account for these corrections. Good agreement with experimental results was obtained, the discrepancy between experiment and theory being reduced to about 8 percent. The adjustment of the ligand oxygen charges and the expansion of the radial wave functions proved to be the most important modifications tested in obtaining the fit.

CONTENTS

FIGURES

TABLES

TABLES (Cont'd)

1. INTRODUCTION

In a previous report[1*] (hereafter referred to as I), we presented the results of a series of measurements of the optical and Zeeman spectra of trivalent ytterbium (Yb^{3+}) doped into the following members of the scheelite family of crystalline hosts: cadmium molybdate ($CdMoO_4$), calcium tungstate ($CaWO_4$), calcium molybdate ($CaMoO_4$), strontium tungstate ($SrWO_4$), strontium molybdate ($SrMoO_4$), lead tungstate ($PbWO_4$), lead molybdate ($PbMoO_4$), barium tungstate ($BaWO_4$), and lithium yttrium fluoride ($LiYF_4$). Measurements were made at temperatures varying from below the lambda point of liquid helium up to room temperature on samples with impurity ion concentrations varying from 0.05 to 4.0 percent Yb. The results were the identification of the electronic transitions, both absorption and fluorescence, and the measurement of the g factors of the lowest J = 5/2 state. These results are given in tables 3 and 4 of I.

The objective of this report is to take these experimental results and from them derive a self-consistent set of crystal-field parameters. Following this calculation, using the conventional approach of the electrostatic point charge model, we calculate a similar set of crystal-field parameters to compare with the experimentally determined ones. Initially, the agreement is poor, as might be expected from the results of previous works[2-5] on the subject. We then discuss modifications to the point charge model that take into account phenomena that may be occurring in the lattice. These modifications include (1) adjustment of the ligand charges to account for the covalent nature of the heavy metal tetrahedra, (2) expansion of the 4f radial wave functon (nephelauxetic effect), and (3) reduction of the ligand distance to

*See numbered references in Literature Cited Section, pp. 34,35.

account for local distortion in the lattice due to the size discrepancy between the Yb^{3+} ion and the normal cation. These modificatons, particularly accounting for the nephelauxetic effect, improve the fit to experiment.

2. DETERMINATION OF EXPERIMENTAL CRYSTAL-FIELD PARAMETERS

The trivalent ytterbium ion has a $4f^{13}$ configuration, which is split by the spin-orbit interaction into two states, $^2F_{5/2}$ and $^2F_{7/2}$, the latter having the Hund's rule ground state. These two states are then split into seven levels, each doubly degenerate (Kramer's degeneracy), by the electric field of the various ions that make up the lattice in which the Yb^{3+} is imbedded. Group theory predicts that, for an S_4 crystalline field, the composition of the two spin-orbit states will be $2\Gamma_{5,6} + 2\Gamma_{7,8}$ for the J = 7/2 level and $2\Gamma_{5,6} + \Gamma_{7,8}$ for the J = 5/2 level, thus giving a total of seven states.

The Hamiltonian representing the crystal field can be written as a multipole expansion of an electrostatic field expressed in terms of spherical tensors. In the notation of Wybourne,[6] this becomes

$$V_c = \sum_{n,m} B_n^{m\dagger} C_n^m + \lambda\left(\vec{S}\cdot\vec{L}\right) \quad , \tag{1}$$

where the coefficients of the tensors are called crystal-field parameters. The second term represents the spin-orbit interaction and, to a first approximation, could be ignored since the average Stark splitting is 300 to 500 cm^{-1} compared with ~10,000 cm^{-1} spin-orbit splitting. Thus, J-mixing has little effect on the energy levels. However, we do include the spin-orbit term since it was found that J-mixing has a profound effect on the g factors.

The sum in equation (1) can be written explicitly as follows. First, for a lanthanide rare earth ($4f^n$ configuration), the sum can be cut off at n = 6 by the triangle rule, which governs the addition of angular momenta. Then by observing which spherical tensors (proportional to spherical harmonics) are compatible with the S_4 symmetry of the crystal field, we see that the series reduces to terms involving C_2^0, $C_3^{\pm 2}$, C_4^0, $C_4^{\pm 4}$, $C_5^{\pm 2}$, C_6^0, and $C_6^{\pm 4}$. Since the wave functions have odd parity, parity considerations of the matrix elements eliminate the two odd crystal-field terms, $C_3^{\pm 2}$ and $C_5^{\pm 2}$. Finally, the overall phase can be adjusted so that $B_4^{\pm 4}$ is real. This adjustment reduces the Hamiltonian to seven terms with seven parameters to be determined:

$$V_c = B_2^0 C_2^0 + B_4^0 C_4^0 + B_4^4 C_4^4 + B_6^0 C_6^0 + \left(\mathrm{Re}\ B_6^4 + \mathrm{Im}\ B_6^4\right) C_6^4 + \lambda\left(\vec{S}\cdot\vec{L}\right) \quad . \quad (2)$$

For Yb^{3+} with a $4f^{13}$ configuration, the wave functions are for a single hole. The evaluation of the radial parts of the matrix elements for V_c involve terms in r^n, and these terms have been calculated by Freeman and Watson.[7] The angular terms are the usual hydrogenic functions. Intermediate coupled states are required, in general, for the rare earth ions since L and S are not good quantum numbers due to the spin-orbit interaction. However, for Yb^{3+}, there is only one term (^2F); thus, this consideration becomes academic. The wave functions used are the same ones calculated by Pappalardo and Wood[8] (except for a correction of the phase in the J = 5/2 states). The 14 × 14 perturbation matrix formed by these wave functions and the Hamiltonian of equation (2) can be reduced to two identical 4 × 4 matrices and two identical 3 × 3 matrices, the former representing the four doubly degenerate J = 7/2 states and the latter representing the three doubly degenerate J = 5/2 states.

Complete diagonalization of the contracted 7 × 7 matrix, fitting of a set of crystal-field and spin-orbit parameters to the experimental data, and calculation of the eigenvalues, wave functions, and g factors were all accomplished by a computer program written by N. Karayianis of the Harry Diamond Laboratories and revised by this author. The program accepted the seven energy levels and the parallel g factors of the lowest J = 5/2 and J = 7/2 states as input. From these, it formed the perturbation matrix and diagonalized it by successive rotations. The resulting eigenvalues were functions of the six crystal-field parameters and λ, the spin-orbit parameter, which then had to be fitted by a parabolic, least squares, iteration subroutine. Goodness of fit was determined by minimizing a quality factor, Q, which is a weighted root mean square deviation. This quality factor is

$$Q = \left(\frac{1}{n} \sum_{i=1}^{n} \frac{X_i^{exp} - X_i^{calc}}{\Delta X_i^{exp}} \right)^{1/2} , \qquad (3)$$

where X_i^{exp} and X_i^{calc} are the experimental and calculated values of the energy levels and g factors to be compared, and ΔX_i^{exp} is the experimental error for these quantities, which is used as a weighting factor. Where X represents a g factor, ΔX contains an additional factor of 100, which causes the Q for the g factors to be of the same order of magnitude as the Q for the energy levels.

In many cases, the selection of spectral lines (energy levels) giving a good fit was not unique. Equally good fits could be obtained in some cases by moving the selection of the S_4 spectral line by as much as 25 cm^{-1}. This uncertainty caused a problem in identifying the electronic transitions, but it also led to a deeper insight into the nature

of the problem. When the matrix is diagonalized, the resulting expressions relating the energy levels to the crystal-field parameters are not solvable analytically. Even for no J-mixing, an attempt to solve exactly the set of equations failed because they were nonlinear, coupled, and probably underdetermined. The addition of J-mixing increases the underdetermined nature of the problem. Thus, it is conceivable that the computer program will calculate small values of Q for more than one set of choices of the seven S_4 lines.

The experimental methods actually used to identify the transitions are discussed in I. The spectral lines and the *g* factors tabulated in I were entered into the program, and the results are shown in table 1; the crystal field and the spin-orbit parameters for the nine lattices will reproduce the energy levels and g factors. As shown in I, there were some highly structured groups of lines in the spectra; by selecting different peaks within each group as the S_4 line, the values of the B_n^m changed. This variation in the B_n^m as the choice of the S_4 lines is varied among the peaks of each group is represented by the errors given in table 1. No error is given for imaginary (Im) B_6^4 values since the variation was very large. The values of this parameter are presented for completeness only and could probably be set to zero or any other value within several orders of magnitude with no change in the results.

TABLE 1. FITTED CRYSTAL-FIELD PARAMETERS FOR NINE SCHEELITE CRYSTALS

B_n^m	$CdMoO_4$	$CaWO_4$	$CaMoO_4$	$SrWO_4$	$SrMoO_4$	$PbWO_4$	$PbMoO_4$	$BaWO_4$	$LiYF_4$
B_2^0	427^{+9}_{-11}	446^{+63}_{-53}	494^{+5}_{-68}	467^{+71}_{-88}	399^{+24}_{-57}	414^{+20}_{-25}	399^{+23}_{-36}	404^{+57}_{-15}	281^{+40}_{-50}
B_4^0	-558^{+28}_{-22}	-538^{+20}_{-59}	-520^{+21}_{-34}	-360^{+39}_{-22}	-307^{+0}_{-54}	-340^{+11}_{-20}	-311^{+22}_{-69}	-262^{+0}_{-60}	-556^{+34}_{-20}
B_4^4	839^{+54}_{-25}	776^{+46}_{-186}	719^{+79}_{-114}	739^{+110}_{-17}	796^{+49}_{-91}	752^{+68}_{-54}	767^{+54}_{-87}	661^{+22}_{-117}	569^{+53}_{-36}
B_6^0	45^{+14}_{-21}	-11^{+27}_{-38}	32^{+15}_{-189}	-29^{+14}_{-80}	-60^{+12}_{-77}	-51^{+21}_{-32}	-39^{+16}_{-76}	-140^{+17}_{-54}	-106^{+100}_{-97}
Re B_6^4	460^{+76}_{-67}	452^{+402}_{-164}	552^{+147}_{-152}	337^{+0}_{-148}	273^{+78}_{-102}	306^{+21}_{-117}	324^{+84}_{-103}	269^{+127}_{-168}	840^{+200}_{-100}
Im B_6^4	-325	518	1	384	310	506	216	499	953
λ	-2902^{+1}_{-3}	-2903^{+2}_{-3}	-2900^{+4}_{-5}	-2904^{+3}_{-3}	-2902^{+3}_{-7}	-2903^{+4}_{-1}	-2901^{+3}_{-4}	-2903^{+0}_{-2}	-2897^{+4}_{-5}

Note: + and - values indicate error limits.

This characteristic of Im B_6^4 was explained when a series of plots was made showing the variation of the energy levels when five of the six crystal parameters are held constant and the sixth is varied by ±500 cm^{-1} about its best fit value. Two of these plots are shown as an example superimposed in figure 1. For $CaWO_4$, the three levels of the J = 5/2 manifold are plotted as a function of B_2^0 and B_6^0. The slope of the lines, which is a direct measure of the dependence of the energy levels on each crystal-field parameter, is considerably greater when B_2^0 is varied than when B_6^0 is varied. This difference illustrates the general result in which it was found that the energy levels were from two to seven times more dependent upon the B_2^0, B_4^0, and B_4^4 values than they were on the sixth order terms. In other words, a large fluctuation in the value of a sixth order parameter would have a negligible effect on the spectra, but a small change in a second or fourth order

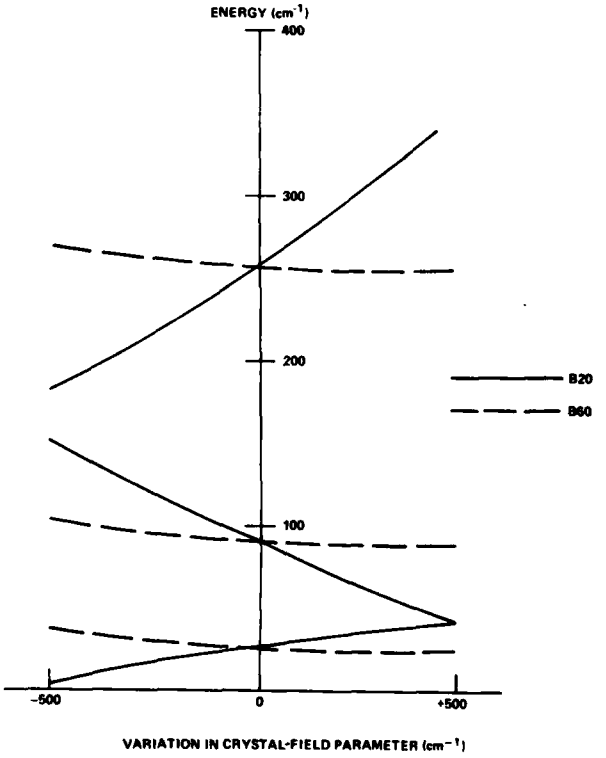

Figure 1. Dependence of $CaWO_4$ J = 5/2 manifold on B_2^0 and B_6^0.

term would cause large shifting in the spectral lines. The spectrum is almost completely independent of the value of Im B_6^4. For this reason, in the following attempt to reproduce the crystal-field parameters from a theoretical model, only the second and fourth order terms are considered, whereas the sixth order parameters are allowed to fall where they may.

3. POINT CHARGE MODEL CALCULATIONS

Let us consider the point charge model in which the basic premise is that the impurity ion bearing a charge (which for the $4f^{13}$ configuration of Yb^{3+} is +e) is subjected to the electric field due to the surrounding ions of the lattice. At a point R from the ion, this lattice charge distribution is $\rho(R)$. If the position of the +e charge of the ion is at the ionic radius, r, then the crystal-field potential at that point can be expressed as

$$V(r) = \int \frac{e\rho(R)}{|\vec{R} - \vec{r}|} d\tau' \qquad (4)$$

$$= \int \sum_{n,m} \frac{4\pi e}{2n+1} \rho(R) \frac{r_<^n}{r_>^{n+1}} Y_n^{m*}(\theta',\phi') Y_n^m(\theta,\phi)\, d\tau' \quad ,$$

where (R,θ',ϕ') and (r,θ,ϕ) are the position coordinates of a point in the lattice charge distribution, $\rho(R)$, and the $4f^{13}$ electrons, respectively; $d\tau'$ indicates that the integration is over the lattice charge distribution; and $r_<$ is the lesser and $r_>$ is the greater of r and R. We

will assume for the present that all of $\rho(R)$ is external to the impurity ion and thus $R > r$. Also, we define spherical tensors to be of the form

$$C_n^m = \sqrt{\frac{4\pi}{2n+1}}\, Y_n^m \quad .$$

Now we can write the crystal-field potential as

$$V(r) = \sum_{n,m} \left[e \int \frac{\rho(R)}{R^{n+1}} C_n^{m*}(\theta',\phi')\, d\Omega' \right] r^n C_n^m(\theta,\phi) \tag{5}$$

$$= \sum_{n,m} A_n^{m\dagger} r^n C_n^m \tag{6}$$

$$= \sum_{n,m} V_n^{m\dagger} C_n^m \quad , \tag{7}$$

where the V_n^m are the calculated equivalents of the experimental crystal-field parameters, the B_n^m. In practice, there is an additional factor in equation (6), so that V_n^m is written

$$V_n^m = A_n^{m\dagger} r^n \left(1 - \alpha_n\right) \quad . \tag{8}$$

In this equation, α_n is a shielding factor that represents the extent that the $5s^2 5p^6$ electrons modify the field at the 4f electrons due to the lattice ions. A_n^m is the electrostatic potential due to the ions of

the crystal at the 4f electrons. Thus, the term $r^n(1 - \alpha_n)$ pertains to the impurity ion, while A_n^m relates to the lattice.

The α_n have been calculated by Sternheimer et al[9] for Pr^{3+} and Tm^{3+}, from which we can obtain approximate values for Yb^{3+} by extrapolation. The second factor of the V_n^m is r^n, which upon forming the matrix elements becomes the expectation value $\langle r^n \rangle$. The calculation of the $\langle r^n \rangle$ for free trivalent rare earth ions has been done by Freeman and Watson[7] using Hartree-Fock methods.

The lattice sums were calculated by changing the integral equation (5) to a sum,

$$A_n^m = e \sum_i \frac{q_i}{R_i^{n+1}} \sqrt{\frac{(n-m)!}{(n+m)!}} \; Y_n^m(\theta_i', \phi_i') \quad . \tag{9}$$

This expression treats the charge distribution $\rho(R)$ in equation (5) as a set of discrete point charges, $q_i e$, and sums over all i of them at their positions $(R_i, \theta_i', \phi_i')$. The Y_n^m are spherical harmonics as defined by Rose or Edmonds.[10,11] Equation (9) can be reexpressed in rectilinear coordinates (x,y,z) with the substitution site taken as the origin. The coordinates of any ion R_i (x_i, y_i, z_i) can be expressed as functions of the nearest neighbor oxygen coordinates (x_O, y_O, z_O). Using equation (9) in equation (8), along with the values of $\langle r^n \rangle$ and $(1 - \alpha_n)$, we calculated values of V_n^m with the aid of a computer program written by C. A. Morrision and N. Karayianis of the Harry Diamond Laboratories and revised by this author. The program performs the lattice sums of equation (9) over all points in the lattice for as many "shells," that is, layers of unit cells, surrounding a particular impurity ion, as desired to obtain convergence.

Before discussing the results of the summing program, however, it is necessary to discuss the nature of this input to the program. Beginning with oxygen coordinates, it has been pointed out in numerous places in the literature (for example, Burns[12]) that small uncertainties in the oxygen coordinates can result in large variations in the calculated values of the A_n^m. This result was indeed borne out by the calculations in this work. Table 2 collects the oxygen (or fluorine) coordinates for all the crystals studied and gathered from various authors. For example, in $CaWO_4$ there are seemingly small discrepancies between the values given by Kay et al[13] and Zalkin and Templeton[14] and those given by Wyckoff.[15] However, they result in a factor of 2 difference in A_2^0 and A_4^4 and a factor of 10 difference in A_4^0. Since there is a much higher degree of accuracy in the neutron diffraction studies of Kay et al (which also agree with the x-ray studies of Zalkin and Templeton), the data of Kay et al are chosen as the preferred set. Likewise, the neutron diffraction studies of Gurmen, Daniels, and King[16] on $CaMoO_4$, $SrWO_4$, $SrMoO_4$, $BaWO_4$; of King on $LiYF_4$; and of Leciejewicz[17] on $PbMoO_4$ have been used rather than Wyckoff's data. There are no available neutron diffraction values of the oxygen coordinates for $CdMoO_4$ or $PbWO_4$; thus, the sums for these lattices were not carried out.

The lattice sums were carried out by locating each type of lattice site with a position vector as follows:

$$R = a\left\{\left[X\left(x_o,y_o,z_o\right) + n_x\right]^2 + \left[Y\left(x_o,y_o,z_o\right) + n_y\right]^2 + \frac{c^2}{a^2}\left[Z\left(x_o,y_o,z_o\right) + n_z\right]^2\right\}^{1/2} , \tag{10}$$

TABLE 2. SCHEELITE COORDINATES

Crystal	Reference	Type of measurement	x_O	y_O	z_O
$CaWO_4$	a	X-ray	0.25 ± 0.02	0.11 ± 0.02	0.07 ± 0.015
	b	X-ray	0.2415 ± 0.0014	0.1504 ± 0.0013	0.086 ± 0.0006
	c*	Neutron	0.2413 ± 0.0005	0.1511 ± 0.0006	0.086 ± 0.0001
$CaMoO_4$	a	X-ray	0.25 ± 0.02	0.15 ± 0.02	0.075 ± 0.015
	d*	Neutron	0.2430 ± 0.0010	0.1459 ± 0.0009	0.030 ± 0.0004
$SrWO_4$	a	X-ray	0.25 ± 0.02	0.14 ± 0.02	0.075 ± 0.015
	d*	Neutron	0.2370 ± 0.0008	0.1387 ± 0.0007	0.0815 ± 0.0003
$SrMoO_4$	a	X-ray	0.25 ± 0.02	0.14 ± 0.02	0.075 ± 0.015
	d*	Neutron	0.2378 ± 0.0010	0.1353 ± 0.0008	0.0800 ± 0.0004
$PbWO_4$	a	X-ray	0.25 ± 0.02	0.13 ± 0.02	0.075 ± 0.015
$PbMoO_4$	a	X-ray	0.247 ± 0.02	0.092 ± 0.02	0.085 ± 0.015
	e*	Neutron	0.2352 ± 0.00068	0.1134 ± 0.00073	0.0439 ± 0.00024
$BaWO_4$	a	X-ray	0.25 ± 0.02	0.11 ± 0.02	0.075 ± 0.015
	d*	Neutron	0.2333 ± 0.0005	0.1214 ± 0.0006	0.0778 ± 0.0002
$LiYF_4$	f*	Neutron	0.2820 ± 0.0011	0.1642 ± 0.0011	0.0815 ± 0.0004

*Values used in lattice sum calculations.
[a] R. W. G. Wyckoff, Crystal Structures, 3, John Wiley and Sons, Inc., New York (1965), 19 ff, taken mainly from L. G. Sillen and A. Nylander, Ark. Kemi. Min. Geol., 17A, No. 4 (1943).
[b] A. Zalkin and D. H. Templeton, J. Chem. Phys., 40 (1964), 501, as quoted in c.
[c] M. I. Kay, B. C. Frazer, and I. Almadovar, J. Chem. Phy., 40 (1964), 504.
[d] E. Gurmen, E. Daniels, and J. S. King, J. Chem. Phys., 55 (1971), 1093-1097.
[e] J. Leciejewicz, Z. Krist., 121 (1965), 158-164.
[f] J. S. King, University of Michigan, private communication.

where a and c are the lattice parameters (given in I) and X, Y, and Z are the site coordinates, which are expressed as functions of the nearest neighbor oxygen or fluorine coordinates (x_O, y_O, z_O). The n are integers that run from zero to some value that is selected to cause the sum to converge. The program is written in such a way that the n are set at their maximum values and stepped down in integral units to zero. In this way, the small contributions from the outer lattice sites are counted first so that they do not lose significance when added to larger inner terms. In general, we set the maximum value of n_z to be half of n_x and n_y since $c \simeq 2a$. This setting allowed us to carry out the lattice sums over a roughly spherical volume. Convergence was determined by carrying out a number of test sums for $CaWO_4$ and varying

the maximum values of the (n_x,n_y,n_z) to determine the point beyond which the lattice sum did not change. The results show that the largest contribution comes from the ligands; the ions farther away contribute relatively little. For A_2^0, a stable value representing convergence is reached by $(n_x,n_y,n_z) = (6,6,3)$, while convergence for the A_4^m and A_6^m sums is achieved by $(n_x,n_y,n_z) = (4,4,2)$. However, as a precaution against small fluctuations--especially in A_2^0, which converges in an oscillatory fashion, it was decided to carry out all sums to $(n_x,n_y,n_z) = (10,10,5)$.

In the tungstate and molybdate scheelites, the bond between the cation and the heavy metal oxide tetrahedron is principally ionic, whereas the tetrehedron itself is mainly covalent. Thus, the total charge of the tetrahedron is -2.0e. A molecular orbital calculation by Karavelas[18] on the vanadate tetrahedron in a $CaWO_4$-like structure showed that practically all the charge resided on the four oxygen ions; this redistribution of charge leaves the vanadium ion almost neutral. The extrapolated ratio of charge for $(WO_4)^{2-}$ results in -0.53e on the oxygen ion and 0.12e on the tungsten ion. From a suggestion by C. A. Morrison of the Harry Diamond Laboratories, the oxygen charges, q_O, were varied between the limits -0.5e and -2.0e (the tungsten charges were varied between the limits 0.0 and +6.0) in an attempt to find a good calculated fit to the experimental data. For $LiYF_4$, the $(LiF_4)^{3-}$ tetrahedron is not covalent, but ionic. Thus, the charge on the fluorine ion is not expected to vary from its value of -1. (For brevity, we refer to the effective oxygen or fluorine charge, q_O, as a dimensionless number and understand it to be multiplying the electronic charge, e.) In the calculation, the values of $\langle r^n \rangle$ were from Freeman and Watson,[7] and the values of α_n were from Sternheimer et al[9] and are listed in table 3. The effective oxygen charge for $CaWO_4:Yb^{3+}$ that gave the best fit was $q_O = -1.30$. The crystal-field parameters calculated with this charge and also with $q_O = -2.00$ are compared with the experimental values in

table 4. The average discrepancy between the five calculated V_n^m from the respective experimental B_n^m (ignoring Im V_6^4 and Im B_6^4) was 66 percent for q_o = -1.30 and 83 percent for q_o = -2.00. The corresponding average percentage of deviation for three parameters (B_2^0, B_4^0, B_4^4) is given also in table 5.

TABLE 3. $\langle r^n \rangle$ AND α_n USED IN CRYSTAL-FIELD PARAMETER CALCULATIONS

n	$\langle r^n \rangle$[a] (atomic units)	α_n[b]
2	0.613	0.533
4	0.960	0.088
6	3.104	-0.043

[a] A. J. Freeman and R. E. Watson, Phys. Rev., 127 (1962), 2058.

[b] R. M. Sternheimer, M. Blume, and R. F. Peierls, Phys. Rev., 173 (1968), 376.

TABLE 4. LATTICE SUMS OF DIFFERENT STUDIES

A_n^m	$CaWO_4$[a]		$PbMoO_4$[b]	
	Eremin et al[c]	This work	Sengupta and Artman[d]	This work
A_2^0	2880	4029	2420	3916
A_4^0	-342	-359	-200	-196
A_6^0	0.86	-0.52	-0.3	-2
Re A_4^4	-159	-150	-47	-81
Im A_4^4	-200	-237	-73	-198
Re A_6^4	-17	-19	-4	-10
Im A_6^4	-15	-16	-4	-10

[a] Oxygen coordinates from N. I. Kay, B. C. Frazer, and I. Almadovar, J. Chem. Phys., 40 (1964), 504; lattice parameters from A. N. Morozov et al, Opt. Spectrosc. (USSR), 22 (1967), 139; oxygen charge = -2.00.

[b] Oxygen coordinates and lattice parameters from J. Leciejewicz, Z. Krist., 121 (1965), 158-164; oxygen charge = -2.00.

[c] N. V. Eremin et al, Sov. Phys. Solid State, 11 (1970), 1697.

[d] D. Sengupta and J. O. Artman, Phys. B, 1 (1970), 2986-2988.

TABLE 5. AGREEMENT BETWEEN EXPERIMENTAL AND CALCULATED CRYSTAL-FIELD PARAMETERS FOR $CaWO_4$ LATTICE

n	m	B_n^m	V_n^m					
			A	B	C	D	E	F
2	0	446 (-53, +63)	1115	571	578	57	397	445 ± 10
4	0	-538 (-59, +20)	-310	-190	-234	-577	-598	-587 ± 2
4	4	776 (-186, +46)	247	171	227	815	586	581 ± 1
6	0	-11 (-38, +27)	-3	-3	-7	-68	-6	-9.1 ± 0.6
6	Re 4	452 (-164, +402)	78	51	68	494	335	291 ± 1
6	Im 4	518	-23	-29	-5	65	-6	22 ± 0.2
Average deviation of fit of B_2^0, B_4^0, and B_4^4 (%)			94	57	52	33	17.8	11.5

Notes: For $A_n^m \langle r^n \rangle (1 - \alpha_n)$, *A:* $q_0 = -2.00$, $\eta = 1.000$, $K = 0$

B: $q_0 = -1.30$, $\eta = 1.000$, $K = 0$

C: $q_0 = -1.16$, $\eta = 0.942$, $K = 0$

D: $q_0 = -0.53$, $\eta = 0.942$, $K = 0.380$

E: $q_0 = -1.00$, $\eta = 1{,}000$, $K = 0.315$

F: $q_0 = -1.00$, $\eta = 0.942$, $K = 0.250$

+ and - values indicate error limits in B_n^m column.

Concerning the method used in determining the best fit, it was noted that, as an average, the errors in the experimental B_n^m were 9, 9, 13, 19, and 41 percent for B_2^0, B_4^0, B_4^4, B_6^0, and Re B_6^4, respectively. (The error in Im B_6^4 was an order of magnitude or more greater than for the other B_n^m.) Since the reliability of the second and fourth order terms was obviously much greater than that of the sixth order terms, it was decided to fit to B_2^0, B_4^0, and B_4^4 by minimizing a root mean square deviation weighted by the relative experimental error:

$$\sigma = \left[\sum_{n,m} \left(\frac{B_n^m - V_n^m}{B_n^m} \right)^2 \frac{B_n^m}{\Delta B_n^m} \right]^{1/2} ,$$

where the sum is over the three second and fourth order terms. Although σ could be used as a figure of merit, the reported 66- and 83-percent fits were the absolute percentages of difference between V_n^m and B_n^m,

$$\% \text{ difference} = \left| \frac{B_n^m - V_n^m}{B_n^m} \right| \times 100\% \quad , \tag{12}$$

averaged over five parameters, B_2^0, B_4^0, B_4^4, B_6^0, and Re B_6^4. It was believed that, although the routine to obtain a best fit minimized σ, the presentation of the percentage of difference allowed us to visualize the goodness of fit more easily.

The results of two papers dealing with lattice sums of scheelites were examined for comparison with the sums calculated in this work. Sengupta and Artman[19] investigated neodymium, Nd^{3+}, and neptunium, Np^{4+}, in $SrWO_4$, $PbMoO_4$, and $BaMoO_4$. Eremin et al[20] investigated Nd^{3+} in $CaWO_4$, $CdMoO_4$, $SrWO_4$, $PbMoO_4$, and $BaMoO_4$. Their results are compared with our calculations in table 4. We computed these sums for comparison only, using the lattice parameters, the oxygen coordinates, and the oxygen charges that were used in those two papers, and we will show that other values for some of these parameters are preferable. The monopole lattice sums calculated by Eremin et al agree well with ours, except that V_2^0 is only 57 percent of our value. The sums of Sengupta and Artman do not agree with ours, most of ours being higher, particularly A_2^0. Although neither paper details the summing technique, the sums probably had not converged. As is mentioned above, it was found to be necessary to sum from the outside in, so that the significance in the contribution of the outer term is not lost during truncation in the computer. It is suggested that this method may not have been used for those papers. Also, particularly for A_2^0, it is necessary to carry out the sum futher before convergence.

Other questions may be raised concerning the lattice sums calculated in those two papers. Sengupta and Artman[19] admit that the heavy metal tetrahedra are covalently bonded, and thus its charge distribution is altered. However, neither they nor Eremin et al[20] adjust the charges. Furthermore, Eremin et al include the dipolar contributions, but only from the nearest neighbor ions. This may not be a valid treatment since the dipolar contribution from the rest of the lattice may not be negligible. Also, Hutchings and Ray[3] show that the multipolar series converges slowly. In fact, they found the quadrupole term to be comparable to the monopole term. Finally, Eremin et al[20] used the oxygen coordinate data for $CaWO_4$ to calculate the lattice sums for the other four lattices that they treated. In light of the sensitivity of the sums to these coordinates, this treatment must make their calculations for $CdMoO_4$, $SrWO_4$, $PbMoO_4$, and $BaMoO_4$ highly suspect.

4. MODIFICATIONS TO CRYSTAL-FIELD PARAMETER CALCULATIONS

It is obvious from the foregoing that the point charge model, while useful in predicting experimental results in a qualitative manner, is not successful quantitatively. Some suggested modifications to the theory have been proposed including lattice polarization[3] and spatial extension of the lattice points[21] and covalent bonding[23-29] of the rare earth ion in the lattice. These modifications have all involved great calculational difficulties necessitating approximations that, in turn, tend to leave the modification suspect.

Alternatively, we have considered the problem from the point of view that when an Yb^{3+} ion enters a scheelite lattice, certain physical phenomena can take place, and an attempt has been made to account for each effect in a phenomenological way. We must be wary of overparame-

terizing the problem, but we must still account for as many of the physical phenomena occurring as we can. The introduction of these phenomenological corrections is not meant to substitute for more exact calculations, but rather to help determine which effects can give agreement between calculated and experimental crystal-field parameters and to set limits on the magnitude of these effects.

The tungstate or molybdate tetrahedron is a covalent complex, and the charge distribution on it will be varied from what it would be if it were ionic. Thus, the effective oxygen charge, q_O, has been introduced as an adjustable parameter. (The charge on the fluorine ion in $LiYF_4$, however, was not varied.) Varying q_O alone does not provide a good fit. Several other modifications have been considered and are discussed in the following sections.

4.1 Effect of Local Lattice Distortion

A modification was suggested by recent work on lattice distortions around impurity ions in alkali halides and alkali earths.[30-32] Since the size mismatch between the Yb^{3+} ions and the divalent cations is between 8 and 31 percent in the various scheelite lattices, it is expected that the eight ligand oxygen or fluorine ions will tend to collapse somewhat toward the Yb^{3+} ion. Thus, the value of the lattice sums will change, especially since the nearest neighbor contribution has been shown to be the dominant term. There was no a priori knowledge of how far the ligands could be allowed to move. It was calculated that there would be sufficient room between the oxygen ions to allow the ligands to collapse until they butted against the Yb^{3+} ion similar to hard sphere packing. This maximum change in ligand distance would range between 6 and 16 percent. Calculating the crystal-field parameters using a reduced ligand distance $R_O' = \eta R_O$, where for $CaWO_4$ $\eta = 0.942$, we

found a best fit to occur for an effective oxygen charge of $q_O = 1.16$. The five-parameter fit improved to 56 percent. However, although a 6- to 16-percent change in the ligand distance was accepted as "reasonable," there was no way of knowing that this is the true magnitude of the distortion. It is probably safe to say that some distortion does occur, but it may well be less than the maximum, "hard sphere" value since the ligands are part of the covalently bonded, heavy metal tetrahedra and are thus restricted in their motion. Another factor that has not been considered explicitly is that, if the ligands distort, there will probably be distortion, displacement, or rotation of the near-neighbor heavy metal tetrahedra to which they are attached. This effect would change the lattice sums, but such an effect would be smaller than the effect of moving just the ligands. The reasons are that the contribution to the lattice sum from the heavy metal ion and the outer oxygen ions on the nearest tetrahedra is much smaller than that from the ligand oxygen ions because of their greater distance. The amount of motion of the outer ions will be much less than that of the ligands because of the binding of the tetrahedra into the rest of the lattice.

4.2 Effect of Distorton of 4f Radial Wave Function

The next attempt at modifying the point charge model proved to be more successful in providing a good fit to the experimental data. We considered the so-called "nephelauxetic" effect, which has been suggested to occur when a free ion is placed in a crystal. Because of the screening of the 4f electrons by the overlapping charge clouds of the surrounding ligands, the 4f electron wave function tends to be "released" from its nucleus and to expand slightly into the crystal. This effect has been discussed in a number of publications by Jørgensen,[33,34] but there is no quantitative result available that would

indicate the amount of this expansion that we might expect for our system of Yb^{3+} in scheelite. Thus, we have treated the radial wave function as another adjustable parameter as follows.

Freeman and Watson[7] have calculated the 4f radial wave functions for the trivalent rare earths to be of the form

$$P_{4f}(r) = \sum_i C_i r^4 e^{-Z_i/r} \quad , \quad i = 1, 2, 3, 4 \quad , \tag{13}$$

with the normalization condition

$$\int_0^\infty P_{4f}^2(r)\, dr = 1 \quad . \tag{14}$$

For Yb^{3+}, the values of the C_i and Z_i are these:

i	C_i	Z_i
1	15.287	3914.4363
2	8.501	790.99957
3	5.667	90.998364
4	3.126	4.8064115

These yield the values of $\langle r^n \rangle$ given in table 3.

It was apparent by observation that, if the wave function did indeed expand, the values of $\langle r^n \rangle$ would increase and the fit would improve. The criterion for adjusting the wave function was that it should be changed enough to shift the $\langle r^n \rangle$ by the desired amounts, but not so much that the probability, $P^2_{4f}(r)$, of finding a 4f electron at some distance from the nucleus would be radically changed. Having no guidance on how much the wave function should expand, we sought merely to keep it at a minimum. The expansion was accomplished by replacing Z_i in equation (13) by $Z_i' = (1 + K)Z_i$, where K is a constant, and C_i by some new normalization constant, $C_i' = \rho C_i$. K and ρ were chosen the same for all i = 1, 2, 3, 4. The result of simultaneously varying K and the oxygen charge was a notably improved fit. The best fit value of K and ρ for $CaWO_4$ was K = 0.250 and ρ = 0.274. The new wave function parameters were these:

i	$C_i' = 0.274C_i$	$Z_i' = 1.250Z_i$
1	4.189	4893.0454
2	2.329	988.74946
3	1.553	113.74796
4	0.857	6.008014

The 4f charge densities for K = 0, K = 0.160, and K = 0.250 are compared in figure 2. These values represent the range over which K varies for all the lattices examined. The charge density of a 4f electron at the Yb^{3+} radius increases as K increases. The average separation between the calcium and oxygen centers in $CaWO_4$ is about 2.45 Å. Thus, the expanded Yb^{3+} wave function does not protrude too far into the oxygen charge cloud. However, the new values of $\langle r^n \rangle$ for $CaWO_4$ are greatly changed, those being

$$\langle r^2 \rangle = 1.090, \langle r^4 \rangle = 3.035, \text{ and } \langle r^6 \rangle = 17.443 \quad .$$

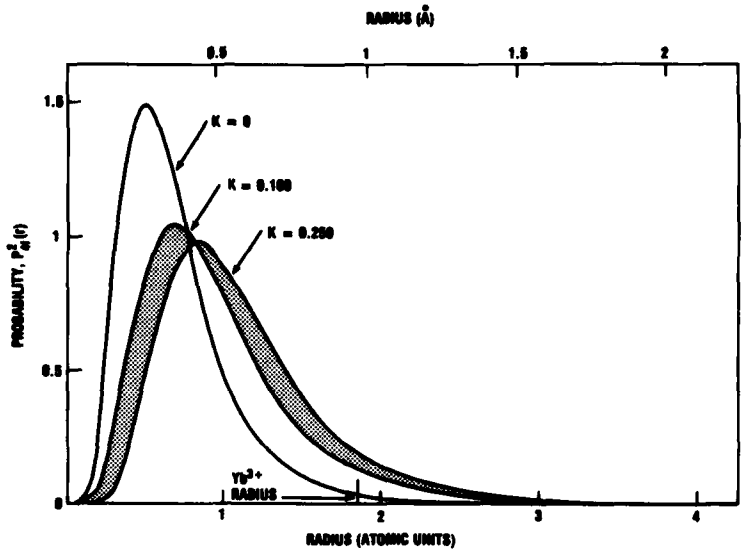

Figure 2. Radial wave functions of 4f electrons of Yb^{3+}.

The best fit for $CaWO_4$ was obtained for an effective oxygen charge of $q_O = -1.00$ with $K = 0.250$. The ligand distance was reduced by $\eta = 0.942$ (5.8 percent) in this case.

The resulting average discrepancy between V_n^m and B_n^m (five-parameter fit) was 17.4 percent. Considering only the errors of B_2^0, B_4^0, and B_4^4, the discrepancy reduces to 11.5 percent. Furthermore, if the experimental error is taken into account, the fit becomes nearly perfect. Without reducing the ligand distance ($\eta = 1$), we can get a good fit also by expanding the wave function somewhat further by changing K from 0.250 to 0.315. The three-parameter fit (second and fourth order terms only) is 17.8 percent without reducing the ligand distance.

4.3 Some Other Possible Effects

There are yet two more possible phenomena. First it is conceivable that the $5s^2 5p^6$ wave functions also would be distorted by the ligands as are the 4f wave functions. This effect would manifest itself by altering the Sternheimer shielding parameters, α_n, n = 2, 4, 6. This effect would probably be small since the 5s and 5p shells are closed, whereas the 4f shell is not. Furthermore, any change in the multiplicative factor $(1 - \alpha_n)$ could be taken up by a change in $\langle r^n \rangle$, which also multiplies A_n^m to get V_n^m.

Second, no calculations have been made to determine the effects of covalency, overlap, or exchange interactions between the ligands and the impurity ions. If meaningful calculations could be made to take these effects into account, it would not be necessary to rely on best-fit criteria to determine the extent of 4f radial wave function expression and local lattice distortion.

5. RESULTS OF CRYSTAL-FIELD PARAMETER CALCULATIONS

The lattice sum program was run for the seven crystals $CaWO_4$, $CaMoO_4$, $SrWO_4$, $SrMoO_4$, $PbMoO_4$, $BaWO_4$, and $LiYF_4$. The ion position for the other two scheelites studied in I were not considered sufficiently accurate for detailed analysis. Various values of q_O, the effective oxygen charge, and K, the radial wave function expansion constant, were tried. The oxygen and fluorine coordinates used are indicated in table 2. The program was run also with and without the ligand distance reduction factor, η. The results are presented in the following tables. Table 6 gives the best fit values of q_O, K, ρ, the resulting $\langle r^n \rangle$, and the ligand distance reduction factor, η. η was not considered as an adjustable parameter, but only as a multiplicative factor of either

1.000 for no local distortion or some value between 0.835 and 0.943, indicating (for the respective lattice) complete relaxation of the ligands into the impurity ion's hard sphere radius.

TABLE 6. LATTICE SUM FITTING PARAMETERS

Crystal	q_O	K	ρ	$\langle r^2 \rangle$	$\langle r^4 \rangle$	$\langle r^6 \rangle$	η
$CaWO_4$	-1.00	0.250	0.27401	1.090	3.035	17.443	0.942
$CaMoO_4$	-1.10	0.240	0.29084	1.062	2.878	16.110	0.943
$SrWO_4$	-1.10	0.200	0.36635	0.958	2.344	11.842	0.893
$SrMoO_4$	-0.90	0.230	0.30846	0.899	2.732	14.895	0.893
$PbMoO_4$	-0.90	0.240	0.29084	1.062	2.878	16.110	0.878
$BaWO_4$	-0.80	0.250	0.27401	1.097	3.035	17.442	0.835
$LiYF_4$	-1.00	0.160	0.43630	0.824	1.929	8.837	0.929

Notes:
q_O is the effective oxygen charge. (For $LiYF_4$, it is the fluorine charge, which does not change from its ionic value.)
K is the radial wave function expansion factor.
ρ is the normalization multiplier for the expanded radial wave function.
η is the ligand distance reduction factor.

Table 5 gives, for $CaWO_4$, a comparison of the experimental crystal-field parameters, B_n^m, with those V_n^m calculated from the point charge model and its modifications. Column A gives the unmodified monopole lattice sum with $q_O = -2.0$ and no correction for ligand distance or wave function expansion (that is, $\eta = 1.000$ and $K = 0$). Column B is similar to column A, but the oxygen charge has been optimized to $q_O = -1.30$. Column C has introduced the reduced ligand distance and has reoptimized the charge to $q_O = -1.16$. Column D gives the fit when q_O is held to -0.53 in accordance with the calculation of Karavelas,[18] and the wave function is allowed to expand. Column E gives the fit obtained with $\eta = 1.000$ and varying q_O and K. The best fit obtained is given in column F, which is similar to the fit in column E, but with $\eta = 0.942$. In columns A, B, and C, the $\langle r^n \rangle$ calculated by Freeman and Watson[7] are used and are given in table 3. In column F, the $\langle r^n \rangle$ used are given in table 6. For

all six columns, the shielding parameters, α_n, were extrapolated from Sternheimer et al[9] and are given in table 3. The progressive improvement in the fit is indicated by the last row in table 5, where the average percentage of deviation of the fit of B_2^0, B_4^0, and B_4^4 is given.

Following this pattern, tables 7 to 13 are similar to table 5, with the results for the other six crystals. Only two sums are shown for each crystal (corresponding to columns A and F in table 5), along with the fitted B_n^m. Table 13 gives the calculated odd lattice sums for completeness. They are given for both $q_o = -2.0$ and the optimized q_o for each crystal.

Considering three parameters (that is, eliminating B_6^0, Re B_6^0, and Im B_4^6), the average difference between the experimental B_n^m and the theoretical V_n^m for seven crystals is 17 percent. If the experimental error in the B_n^m is included, the difference of fit reduces to 8.5 percent.

TABLE 7. AGREEMENT BETWEEN EXPERIMENTAL AND CALCULATED CRYSTAL-FIELD PARAMETERS FOR $CaMoO_4$ LATTICE

n	m	B_n^m	$V_n^m = A_n^m \langle r^n \rangle (1 - \alpha_n)$	
			$q_o = -2.00$, K = 0	$q_o = 1.10$, K = 0.240
2	0	494 (-68, +5)	1054	533 ± 10
4	0	-520 (-34, +21)	-261	-374 ± 2
4	4	719 (-114, +79)	240	590 ± 1
6	0	32 (-189, +15)	-4	-18.2 ± 0.6
6	Re 4	552 (-152, +147)	68	255 ± 1
6	Im 4	1	-20	14.3 ± 0.2
Average deviation of fit of B_2^0, B_4^0, and B_4^4 (%)			54.6	17.3

Note: + and - values indicate error limits in B_n^m column.

TABLE 8. AGREEMENT BETWEEN EXPERIMENTAL AND CALCULATED CRYSTAL-FIELD PARAMETERS FOR $SrWO_4$ LATTICE

n	m	B_n^m	$V_n^m = A_n^m \langle r^n \rangle (1 - \sigma_n)$	
			$q_0 = 2.00$, $K = 0$	$q_0 = -1.10$, $K = 0.200$
2	0	467 (-88, +71)	1086	457 ± 10
4	0	-360 (-22, +39)	-187	-421 ± 2
4	4	739 (-17, +110)	196	489 ± 1
6	0	-29 (-80, +14)	-7	-26 ± 0.6
6	Re 4	337 (-148, +0)	48	172 ± 1
6	Im 4	384	-18	35 ± 0.2
Average deviation of fit of B_2^0, B_4^0, and B_4^4 (%)			60.4	17.7

Note: + and - values indicate error limits in B_n^m column.

TABLE 9. AGREEMENT BETWEEN EXPERIMENTAL AND CALCULATED CRYSTAL-FIELD PARAMETERS FOR $SrMoO_4$ LATTICE

n	m	B_n^m	$V_n^m = A_n^m \langle r^n \rangle (1 - \sigma_n)$	
			$q_0 = -2.00$, $K = 0$	$q_0 = -0.90$, $K = 0.230$
2	0	399 (-57, +24)	1058	374 ± 10
4	0	-307 (-54, +0)	-167	-364 ± 2
4	4	796 (-91, +49)	191	485 ± 1
6	0	-60 (-77, +12)	-6	-37 ± 0.6
6	Re 4	273 (-102, +78)	44	172 ± 1
6	Im 4	310	-17	38 ± 0.2
Average deviation of fit of B_2^0, B_4^0, and B_4^4 (%)			70.5	21.2

Note: + and - values indicate error limits in B_n^m column.

TABLE 10. AGREEMENT BETWEEN EXPERIMENTAL AND CALCULATED CRYSTAL-FIELD PARAMETERS FOR $PbMoO_4$ LATTICE

n	m	B_n^m	$V_n^m = A_n^m \langle r^n \rangle (1 - \sigma_n)$	
			$q_0 = 2.00$, K = 0	$q_0 = -0.98$, K = 0.240
2	0	399 (-36, +23)	1121	377 ± 10
4	0	-311 (-69, +22)	-172	-412 ± 2
4	4	767 (-87, +54)	187	539 ± 1
6	0	-39 (-76, +16)	-6	-40 ± 0.6
6	Re 4	324 (-103, +84)	44	197 ± 1
6	Im 4	216	-18	49 ± 0.2
Average deviation of fit of B_2^0, B_4^0, and B_4^4 (%)			75.5	19.4

Note: + and - values indicate error limits in B_n^m column.

TABLE 11. AGREEMENT BETWEEN EXPERIMENTAL AND CALCULATED CRYSTAL-FIELD PARAMETERS FOR $BaWO_4$ LATTICE

n	m	B_n^m	$V_n^m = A_n^m \langle r^n \rangle (1 - \sigma_n)$	
			$q_0 = -2.00$, K = 0	$q_0 = -0.80$, K = 0.250
2	0	404 (-15, +57)	1057	371 ± 10
4	0	-262 (-60, +0)	-93	-306 ± 2
4	4	661 (-117, +22)	143	509 ± 1
6	0	-140 (-54, +17)	-7	-69 ± 0.6
6	Re 4	269 (-168, +127)	26	155 ± 1
6	Im 4	499	-13	62 ± 0.2
Average deviation of fit of B_2^0, B_4^0, and B_4^4 (%)			77.1	16.0

Note: + and - values indicate error limits in B_n^m column.

TABLE 12. AGREEMENT BETWEEN EXPERIMENTAL AND CALCULATED CRYSTAL-FIELD PARAMETERS FOR $LiYF_4$ LATTICE

n	m	B_n^m	$V_n^n = A_n^m \langle r^n \rangle (1 - \sigma_n)$	
			$q_0 = -1.00$, K = 0	$q_0 = -1.00$, K = 0.160
2	0	281 (-50, +40)	88	284 ± 10
4	0	-556 (-20, +34)	-133	-432 ± 2
4	4	569 (-36, +53)	232	585 ± 1
6	0	-106 (-97, +200)	-1	-11 ± 0.6
6	Re 4	840 (-100, +200)	52	283 ± 1
6	Im 4	953	-8	35 ± 0.2
Average deviation of fit of B_2^0, B_4^0, and B_4^4 (%)			48.5	14.6

Note: + and - values indicate error limits in B_n^m column.

TABLE 13. CALCULATED VALUES FOR ODD LATTICE SUMS

Crystal	q_0	Re A_3^2	Im A_3^2	Re A_5^2	Im A_5^2
$CaWO_4$	-2.00	224	310	-146	16
	-1.00	-45	-234	-93	-8
$CaMoO_4$	-2.00	286	254	-143	14
	-1.10	32	-199	-102	-8
$SrWO_4$	-2.00	284	242	-117	14
	-1.10	-10	-316	-102	-12
$SrMoO_4$	-2.00	317	205	-115	13
	-0.90	-6	-301	-88	-13
$PbMoO_4$	-2.00	320	236	-113	14
	-0.90	-3	-323	-91	-14
$BaWO_4$	-2.00	281	157	-87	11
	-0.80	-8	-349	-83	-17
$LiYF_4$	-1.00	187	-46	-171	1

The greatest error, in general, lies in the n = 6 terms. The reason for this error may be partly that $\langle r^6 \rangle$ is considerably more sensitive to perturbation by the ligand ions than is $\langle r^2 \rangle$ or $\langle r^4 \rangle$. It is more sensitive because the sixth power amplifies the contribution of $\langle r^n \rangle$ of the radial wave function tail, which extends further into the lattice than do the tails of the second and fourth powers.

6. CONCLUSIONS

The point charge model in its basic form does not accurately reproduce the experimental data. However, modifying the theory by including various effects that occur when an impurity ion enters a lattice yields greatly improved results. In particular, accounting for the covalent bonding of the $(WO_4)^{2-}$ and $(MoO_4)^{2-}$ tetrahedra by adjusting the effective oxygen charge and accounting for the expansion of the 4f radial wave function (nephelauxetic effect) seem to be especially useful in fitting the theoretical V_n^m to the experimental B_n^m. The results strongly suggest that 4f wave functions expand radially when the ion is introduced into a solid. Local distortion of the ligand ions may or may not occur. A good fit between calculated and experimental crystal-field parameters is obtained whether or not we assume local distortion. However, neglect of this effect requires the assumption of a greater 4f wave function distortion to obtain an equally good fit to the experimental crystal-field parameters.

Furthermore, adjusting the oxygen charge, considering the local lattice distortion at the ligands, and examining the nephelauxetic effect are all manifestations of the covalent nature of the lattice and the bonding of the impurity ion in the lattice. Nevertheless, they have all been treated in a phenomenological manner and are thus only an approximate approach to the problem. However, rigorous covalency calcu-

lations are usually quite difficult and require assumptions to be made as to the positions and the wave functions of the ions concerned. They are often no more accurate than the phenomenological treatment of this work. The results of this study also confirmed the fact that the positions of the ions in the lattice bear a critical relation to the lattice sums from which the crystal-field parameters are calculated.

ACKNOWLEDGEMENT

The author thanks the following individuals for their many helpful discussions during the course of this work: J. Nemarich, N. Karayianis, C. A. Morrison, J. P. Sattler, and D. E. Wortman of the Harry Diamond Laboratories. Thanks are offered to N. Karayianis and C. A. Morrison for the use of their computer programs and to R. Leavitt for his thoughtful review and comment on the final draft of this report.

LITERATURE CITED

(1) E. A. Brown, Optical Spectra of Yb^{3+} in Crystals with Scheelite Structure, I. Explanation of the Spectra, Harry Diamond Laboratories HDL-TR-1932 (September 1980).

(2) J. S. Margolis, J. Chem. Phys., 35 (1961), 1367.

(3) M. T. Hutchings and D. K. Ray, Proc. Phys. Soc. (London), 81 (1963), 663.

(4) J. J. Pearson, G. F. Herrmann, K. A. Wickersheim, and R. A. Buchanan, Phys. Rev., 159 (1967), 251.

(5) M. T. Hutchings and W. P. Wolf, J. Chem. Phys., 41 (1964), 617.

(6) B. G. Wybourne, Spectroscopic Properties of Rare Earth, John Wiley and Sons, Inc., New York (1965), 164.

(7) A. J. Freeman and R. E. Watson, Phys. Rev., 127 (1962), 2058.

(8) R. Pappalardo and D. L. Wood, J. Mol. Spectrosc., 10 (1963), 81.

(9) R. M. Sternheimer, M. Blume, and R. F. Peierls, Phys. Rev., 173 (1968), 376.

(10) M. E. Rose, Elementary Theory of Angular Momentum, John Wiley and Sons, Inc., New York (1963).

(11) A. R. Edmonds, Angular Momentum in Quantum Mechanics, Princeton University Press, Princeton, NJ (1963).

(12) G. Burns, Phys. Rev., 128 (1962), 2121.

(13) M. I. Kay, B. C. Frazer, and I. Almadovar, J. Chem. Phys., 40 (1964), 504.

(14) A. Zalkin and D. H. Templeton, J. Chem Phys., 40 (1964), 501.

(15) R. W. G. Wyckoff, Crystal Structures, 3, John Wiley and Sons, Inc., New York (1965), 19 ff.

(16) E. Gurmen, E. Daniels, and J. S. King, J. Chem. Phys., 55 (1971), 1092-1097.

(17) J. Leciejewicz, Z. Krist., 121 (1965), 158-164.

(18) S. Karavelas and C. Kikuchi, University of Michigan, Ann Arbor, MI, Technical Report 06029-3-T (1965).

(19) D. Sengupta and J. O. Artman, Phys. Rev. B., 1 (1970), 2986.

(20) M. V. Eremin, I. N. Kurkin, O. I. Mar'yakhina, and L. Ya. Shekun, Sov. Phys. Solid State, 11 (1970), 1697.

(21) G. Burns, J. Chem. Phys., 42 (1965), 377.

(22) R. E. Watson and A. J. Freeman, Phys. Rev., 156 (1967), 251.

(23) M. M. Ellis and P. J. Newman, Phys. Lett., 21 (1966), 508.

(24) M. M. Ellis and P. J. Newman, Phys. Lett., 23 (1966), 46.

(25) M. M. Ellis and P. J. Newman, J. Chem. Phys., 47 (1967), 1986.

(26) M. M. Ellis and P. J. Newman, J. Chem. Phys., 47 (1967), 4133.

(27) M. M. Ellis and P. J. Newman, J. Chem. Phys., 49 (1968), 4037.

(28) M. M. Ellis and P. J. Newman, J. Chem. Phys., 50 (1969), 1077.

(29) M. M. Ellis and P. J. Newman, J. Chem. Phys., 52 (1970), 1340.

(30) B. G. Dick and T. P. Das, Phys. Rev., 127 (1962), 1053.

(31) T. P. Das, Phys. Rev., 140 (1965), A1957.

(32) R. J. Quigley and T. P. Das, Phys. Rev., 164 (1967), 1185.

(33) C. J. Jφrgensen, Orbitals in Atoms and Molecules, Academic Press, New York (1962).

(34) C. J. Jφrgensen, Absorption Spectra and Chemical Bonding in Complexes, Addison-Wesley Publishing Co., Inc., Reading, MA (1962).

DISTRIBUTION

DEFENSE DOCUMENTATION CENTER
CAMERON STATION, BUILDING 5
ATTN DDC-TCA (12 COPIES)
ALEXANDRIA, VA 22314

COMMANDER
US ARMY RSCH & STD GP (EUR)
ATTN CHIEF, PHYSICS & MATH BRANCH
BOX 65
FPO NEW YORK 09510

COMMANDER
US ARMY MATERIEL DEVELOPMENT & READINESS COMMAND
ATTN DRCDE, DIR FOR DEV & ENG
ATTN DRCDMD-ST
ATTN DRCLDC (JAMES BENDER)
5001 EISENHOWER AVENUE
ALEXANDRIA, VA 22333

COMMANDER
US ARMY ARMAMENT MATERIEL READINESS COMMAND
ATTN DRSAR-ASF, FUZE & MUNITIONS SPT DIV
ATTN DRSAR-LEP-L, TECHNICAL LIBRARY
ROCK ISLAND ARSENAL
ROCK ISLAND, IL 61299

COMMANDER
US ARMY MISSILE & MUNITIONS CENTER & SCHOOL
ATTN ATSK-CTD-F
REDSTONE ARSENAL, AL 35809

DIRECTOR
US ARMY MATERIEL SYSTEMS ANALYSIS ACTIVITY
ATTN DRXSY-MP
ABERDEEN PROVING GROUND, MD 21005

TELEDYNE BROWN ENGINEERING
CUMMINGS RESEARCH PARK
ATTN DR. MELVIN L. PRICE, MS-44
HUNTSVILLE, AL 35807

ENGINEERING SOCIETIES LIBRARY
ATTN ACQUISITIONS DEPARTMENT
345 EAST 47TH STREET
NEW YORK, NY 10017

US ARMY ELECTRONICS TECHNOLOGY
& DEVICES LABORATORY
ATTN DELET-DD
ATTN DELET-MJ (DR. HAROLD JACOBS)
FORT MONMOUTH, NH 07703

DEPARTMENT OF DEFENSE
OUSDR&E
ATTN DR. GEORGE G. GOMOTA
WASHINGTON, DC 20301

DIRECTOR
DEFENSE ADVANCED RESEARCH PROJECTS AGENCY
ARCHITECT BLDG
ATTN DEPUTY DIRECTOR FOR RESEARCH
ATTN DR. DOUGLAS H. TANIMOTO
1400 WILSON BLVD
ARLINGTON, VA 22209

DIRECTOR
DEFENSE NUCLEAR AGENCY
ATTN APTL, TECH LIBRARY
ATTN DR. EDWARD CONRAD
ATTN DR. ROBERT OSWALD
WASHINGON, DC 20305

UNDER SECRETARY OF DEFENSE FOR RES AND
ENGINEERING
ATTN TECHNICAL LIBRARY (3C128)
WASHINGTON, DC 20301

OFFICE, CHIEF OF RESEARCH,
DEVELOPMENT, & ACQUISITION
DEPARTMENT OF THE ARMY
ATTN DAMA-AR, DR. M. E. LASSER
ATTN DAMA-ARZ-D, DR. F. VERDERAME
WASHINGTON, DC 20310

COMMANDER
US ARMY RESEARCH OFFICE (DURHAM)
ATTN DR. ROBERT LONTZ (2 COPIES)
PO BOX 12211
RESEARCH TRIANGLE PARK, NC 27709

COMMANDER
ARMY MATERIALS & MECHANICS RESEARCH
CENTER
ATTN DRXMR-TL, TECH LIBRARY BR
WATERTOWN, MA 02172

COMMANDER
NATICK LABORATORIES
ATTN DRXRES-RTL, TECH LIBRARY
NATICK, MA 01762

COMMANDER
USA FOREIGN SCIENCE & TECHNOLOGY CENTER
ATTN DRXST-BS, BASIC SCIENCE DIV
FEDERAL OFFICE BUILDING
220 7TH STREET NE
CHARLOTTESVILLE, VA 22901

DIRECTOR
US ARMY BALLISTICS RESEARCH LABORATORY
ATTN DRXBR, DIRECTOR, R. EICHELBERGER
ATTN DRXBR-TB, FRANK J. ALLEN
ATTN DRXBR, TECH LIBRARY
ATTN DRDAR-TSB-S (STINFO)
ABERDEEN PROVING GROUND, MD 21005

DIRECTOR
ELECTRONIC WARFARE LABORATORY
ATTN TECHNICAL LIBRARY
ATTN J. CHARLTON
ATTN DR. HIESLMAIR
ATTN J. STROZYK
ATTN DR. E. J. TEBO
FT MONMOUTH, NJ 07703

DIRECTOR
NIGHT VISION & ELECTRO-OPTICS LABORATORY
ATTN TECHNICAL LIBRARY
ATTN R. BUSER
ATTN G. JONES
FT BELVOIR, VA 22060

COMMANDER
ATMOSPHERIC SCIENCES LABORATORY
ATTN TECHNICAL LIBRARY
WHITE SANDS MISSILE RANGE, NM 88002

DIRECTOR
DEFENSE COMMUNICATIONS ENGINEERING CENTER
ATTN PETER A, VENA
1860 WIEHLE AVE
RESTON, VA 22090

COMMANDER
US ARMY MISSILE COMMAND
ATTN DRDMI-TB, REDSTONE SCI INFO CENTER
ATTN DRCPM-HEL, DR. W. B. JENNINGS
ATTN DR. J. P. HALLOWES
ATTN T. HONEYCUTT
REDSTONE ARSENAL, AL 35809

COMMANDER
EDGEWOOD ARSENAL
ATTN SAREA-TS-L, TECH LIBRARY
EDGEWOOD ARSENAL, MD 21010

COMMANDER
US ARMY ARMAMENT RES & DEV COMMAND
ATTN DRDAR-TSS, STINFO DIV
DOVER, NJ 07801

COMMANDER
US ARMY TEST & EVALUATION COMMAND
ATTN TECH LIBRARY
ABERDEEN PROVING GROUND, MD 21005

COMMANDER
US ARMY ABERDEEN PROVING GROUND
ATTN STEAP-TL, TECH LIBRARY, BLDG 305
ABERDEEN PROVING GROUND, MD 21005

COMMANDER
ATTN DRSEL-WL-MS, ROBERT NELSON
WHITE SANDS MISSILE RANGE, NM 88002

COMMANDER
GENERAL THOMAS J. RODMAN LABORATORY
ROCK ISLAND ARSENAL
ATTN SWERR-PL, TECH LIBRARY
ROCK ISLAND, IL 61201

COMMANDER
US ARMY CHEMICAL CENTER & SCHOOL
FORT MCCLELLAN, AL 36201

COMMANDER
NAVAL OCEAN SYSTEMS CENTER
ATTN TECH LIBRARY
SAN DIEGO, CA 92152

COMMANDER
NAVAL SURFACE WEAPONS CENTER
ATTN WX-40, TECHNICAL LIBRARY
WHITE OAK, MD 20910

DIRECTOR
NAVAL RESEARCH LABORATORY
ATTN CODE 2620, TECH LIBRARY BR
ATTN CODE 5554, DR. LEON ESTEROWITZ
ATTN CODE 5554, DR. S. BARTOLI
ATTN CODE 5554, R. E. ALLEN
WASHINGTON, DC 20390

COMMANDER
NAVAL WEAPONS CENTER
ATTN CODE 753, LIBRARY DIV
CHINA LAKE, CA 93555

OFFICE OF NAVAL RESEARCH
ATTN DR. V. O. NICOLAI
ARLINGTON, VA 22217

COMMANDER
AF ELECTRONICS SYSTEMS DIV
ATTN TECH LIBRARY
L. G. HANSCOM AFB, MA 01730

DEPARTMENT OF COMMERCE
NATIONAL BUREAU OF STANDARDS
ATTN LIBRARY
ATTN DR. W. BROWNER
ATTN H. S. PARKER
WASHINGTON, DC 20234

DIRECTOR
LAWRENCE RADIATION LABORATORY
ATTN DR. MARVIN J. WEBER
ATTN DR. HELMUT A. KOEHLER
LIVERMORE, CA 94550

NASA GODDARD SPACE FLIGHT CENTER
ATTN CODE 252, DOC SECT, LIBRARY
GREENBELT, MD 20771

DISTRIBUTION (Cont'd)

NASA HEADQUARTERS
ATTN RTE-G (DR. M. SOKOLOSKI)
WASHINGTON, DC 20546

NATIONAL OCEANIC & ATMOSPHERIC ADM
ENVIRONMENTAL RESEARCH LABORATORIES
ATTN LIBRARY, R-51, TECH REPORTS
BOULDER, CO 80302

DIRECTOR
ADVISORY GROUP ON ELECTRON DEVICES
ATTN SECTRY, WORKING GROUP D
201 VARICK STREET
NEW YORK, NY 10013

THE AEROSPACE CORPORATION
THE IVAN A. GETTING LABORATORY
ATTN DR. DEAN T. HODGES
PO BOX 92957
LOS ANGELES, CA 90009

HONEYWELL CORPORATE RESEARCH CENTER
ATTN DR. PAUL W. KRUSE
10701 LYNDALE AVENUE SOUTH
BLOOMINGTON, MN 55420

BOOZ-ALLEN & HAMILTON
ATTN BRUCE M. FONOROFF
ATTN HARRY GIESKE
4330 EAST-WEST HIGHWAY
BETHESDA, MD 20014

CARNEGIE MELLON UNIVERSITY
SCHENLEY PARK
ATTN PHYSICS & EE
DR. J. O. ARTMAN
PITTSBURGH, PA 15213

UNIVERSITY OF MICHIGAN
COLLEGE OF ENGINEERING NORTH CAMPUS
DEPARTMENT OF NUCLEAR ENGINEERING
ATTN DR. CHIHIRO KIKUCHI
ANN ARBOR, MI 48104

CRYSTAL PHYSICS LABORATORY
MASSACHUSETTS INSTITUTE OF TECHNOLOGY
ATTN DR. A. LINZ
ATTN DR. H. P. JENSSEN
CAMBRIDGE, MA 02139

CENTER FOR LASER STUDIES
UNIVERSITY OF SOUTHERN CALIFORNIA
ATTN DR. L. G. DE SHAZER
LOS ANGELES, CA 90007

JOHNS HOPKINS UNIVERSITY
PHYSICS DEPARTMENT
ATTN PROF B. R. JUDD
BALTIMORE, MD 21218

ARGONNE NATIONAL LABORATORY
ATTN DR. W. T. CARNALL
9700 SOUTH CASS AVENUE
ARGONNE, IL 60439

MONTANA STATE UNIVERSITY
PHYSICS DEPT
ATTN PROF RUFUS L. CONE
BOZEMAN, MT 59715

NORTH DAKOTA STATE UNIVERSITY
PYSICS DEPT
ATTN PROF J. GRUBER
FARGO, ND 58102

RARE-EARTH INFORMATION CENTER
ENERGY AND MINERAL RESOURCES RESEARCH INSTITUTE
ATTN DR. KARL GSCHNEIDNER, JR.
IOWA STATE UNIVERSITY
AMES, IA 50011

US ARMY ELECTRONICS RESEARCH
& DEVELOPMENT COMMAND
ATTN TECHNICAL DIRECTOR, DRDEL-CT

HARRY DIAMOND LABORATORIES
ATTN CO/TD/TSO/DIVISION DIRECTORS
ATTN CHIEF, 11000
ATTN CHIEF, 13000
ATTN CHIEF, 15300
ATTN RECORD COPY, 81200
ATTN HDL LIBRARY, (3 COPIES) 81100
ATTN HDL LIBRARY, (WOODBRIDGE) 81100
ATTN TECHNICAL REPORTS BRANCH, 81300
ATTN CHAIRMAN, EDITORIAL COMMITTEE
ATTN FARRAR, R., 13500
ATTN KARAYIANIS, N., 13200
ATTN KULPA, S., 13300
ATTN LEAVITT, R., 13200
ATTN MORRISON, C., 13200
ATTN WORTMAN, D., 13200
ATTN SATTLER, J., 13200
ATTN SIMONIS, G., 13200
ATTN WORCHESKY, T., 13200
ATTN BROWN, E. A., 00210 (25 COPIES)
ATTN CHIEF, 13300
ATTN TOBIN, M., 13200